

miRNAs are important for post transcriptional regulation of mRNAs and earlier reports suggest that specific nuclear encoded miRNAs can translocate to mitochondria under specific stimuli and can regulate translation mitochondrial DNA encoded transcripts[1]. The intranuclear inclusions, pathological hallmark of FXTAS, are known to sequester several RNA binding proteins involved in miRNA biogenesis, including DROSHA and DGCR8 [2]. Further, mass spectroscopy data suggests role of FMRpolyG in sequestration of important mitochondrial localized RNA binding proteins involved in mitochondria RNA processing [3]. Based on these findings, we hypothesize that mitochondrial dysfunctions in premutation carriers is a cause of mitochondrial RNA processing defect, which is mainly due to altered translocation of miRNAs to mitochondria and/or sequestration of important RNA binding proteins involved in regulation of mitochondrial functions. Therefore, miRNA association with mitochondria under expanded CGG repeats transfected condition was analyzed. Further, this study was proposed to identify the possible role of mito-miRNAs in mitochondrial RNA processing and impaired mitochondrial functions in FXTAS.

7.1 Expanded CGG repeats alter miRNAs expression and their association with mitochondria.

Growing evidences suggest that specific miRNAs can be present in specific membrane-bound compartments including secreted vesicles, P bodies, ER membrane and mitochondria[1], [4]–[7]. As miRNAs expression and mitochondrial functions are affected in FXTAS, we investigated the association of miRNAs with mitochondria in premutation condition. Briefly, small RNAs were isolated from mitochondrial fraction and total cell of HEK293 cells transfected with ATG FMRpolyG-GFP, 5'UTR *FMR1* CGG99X and pEGFP-C1. RNA samples were analyzed on Illumina HiSeq platform by following standard method (Fig.7.2A). The RNA sequencing results showed down regulation of a majority of miRNAs in both ATG FMRpolyG-GFP and 5'UTR *FMR1* CGG99X transfected conditions in mitochondrial and total cell fractions (Fig.7.1A,B,C,D), which is consistent with previous studies [19],[35], and validates our experimental strategy. We further confirmed decreased levels of candidate miRNAs in RNAs isolated from brain tissue of individuals with FXTAS compared to control (Fig. 7.1E). Interestingly, high reads of some specific miRNAs from the mitochondrial fractions indicated their enhanced association with mitochondria in premutation conditions (Fig. 7.2B,C). We also observed that some miRNAs showing reduced reads in total cells, were highly enriched in mitochondrial fraction and vice versa in both CGG repeats transected groups (Fig.7.2D,E). Further, there were some miRNAs which showed no significant change in terms of their

abundance in total cell lysates but showed altered pattern of association with mitochondria (Fig 7.2F,G).

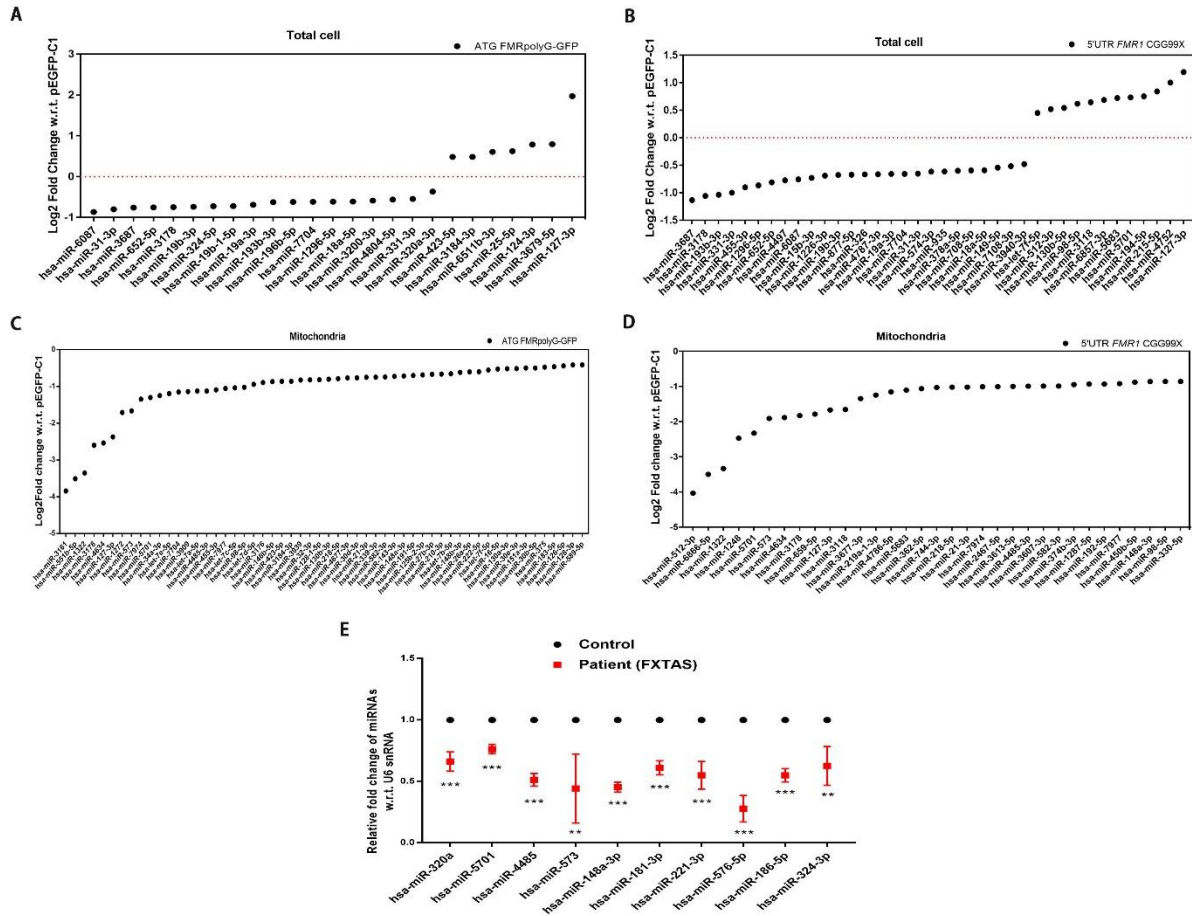


Figure 7.1. Expression of expanded CGG repeats causes differential expression of cellular and mitochondrial miRNAs. List of miRNAs from next generation sequencing data showing altered cellular abundance in HEK293 cells transfected with ATG FMRpolyG-GFP (A) and 5'UTR *FMR1* CGG99X (B) compared to pEGFP-C1. List of miRNAs showing decreased count in mitochondrial fraction (C, D, n=2, for all the listed miRNAs p and $p_{adj} \leq 0.05$). qPCR results showing expression levels of candidate miRNAs from brain tissue of FXTAS patients (n=4) compared to control (n=4), $p > 0.05$ (ns), $p \leq 0.05$ (*), $p \leq 0.01$ (**), $p \leq 0.001$ (***).

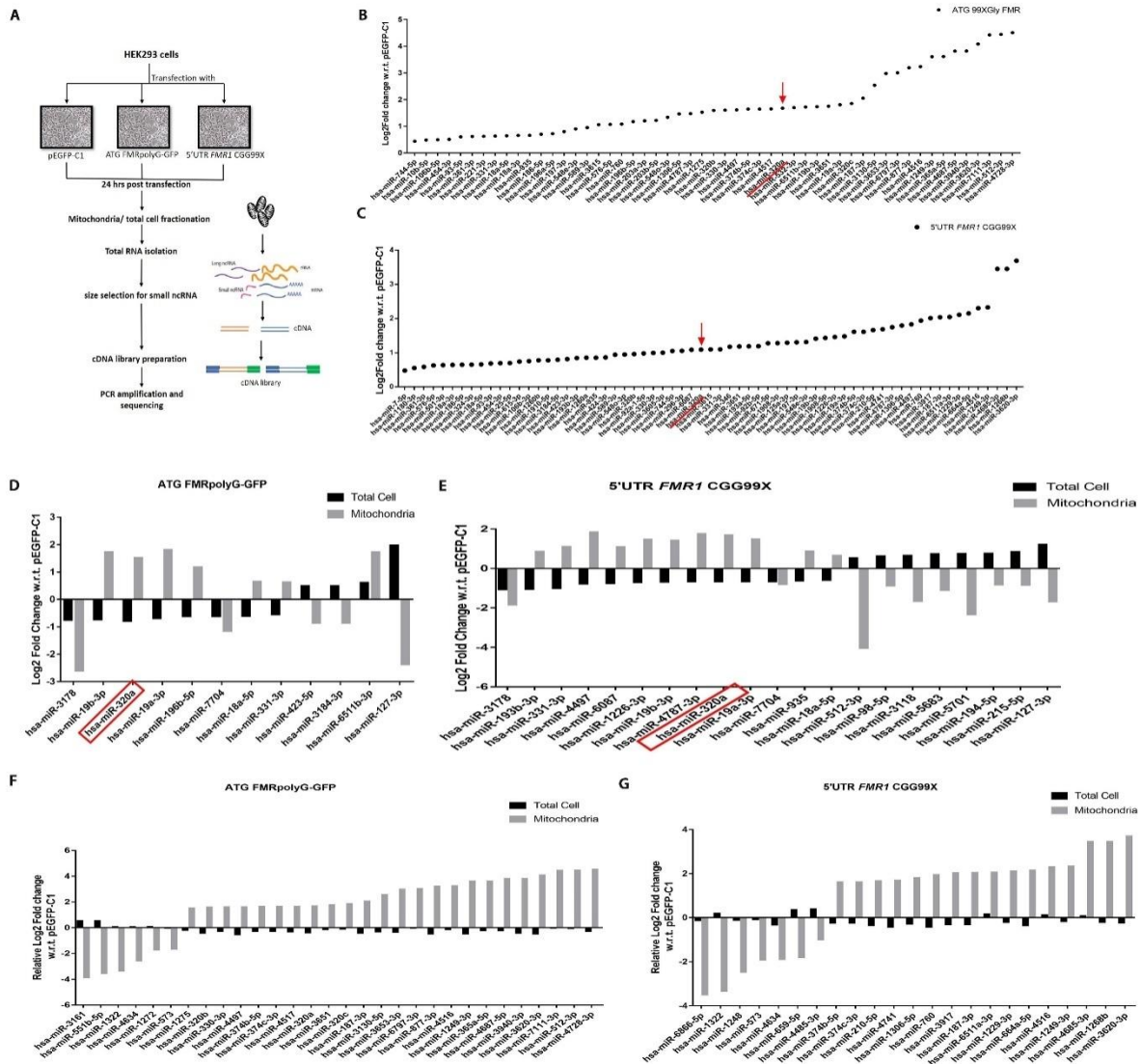


Figure 7.2. FMRpolyG translated due to CGG repeats causes altered pattern of mitochondrial associated miRNAs. Flowchart explaining workflow beginning with transfection of pre-mutation constructs in HEK293 cells followed by mitochondrial fractionation and isolation of RNAs for next generation sequencing (A). NGS analysis showing high enrichment of miRNAs in mitochondrial fraction of HEK293 cells transfected with ATG FMRpolyG-GFP (B) and 5'UTR *FMRI* CGG99X (C) compared to pEGFP-C1. Representative graphs showing opposite enrichment of miRNAs in mitochondrial fraction compared to total cell fraction under ATG FMRpolyG-GFP (D) and 5'UTR *FMRI* CGG99X (E) transfected condition. Comparative analysis for miRNAs enrichment which remained unchanged in total cell fraction while showed altered pattern of association at mitochondria in ATG FMRpolyG-GFP (F) and 5'UTR *FMRI* CGG99X (G) transfected condition. (n=2, for all the listed miRNAs p and $p_{adj} \leq 0.05$).

The putative targets of these miRNAs associated with mitochondria in FXTAS condition were enlisted using miRDB [9]. The targets were clustered into different useful groups such as OMIM enriched tissue, biological process and cellular compartments using DAVID platform [10]. The bioinformatics analysis for tissue enrichment showed that 37% and 40% of the targets of mito-miRs from transfected ATG FMRpolyG-GFP (Fig. 7.3A) and 5'UTR *FMRI* (CGG)^{99X} (Fig.7.3B) were associated with brain, respectively. Clustering based on biological process indicates involvement of targets in nervous system development, mRNA processing, protein ubiquitination and other neuronal functions (Fig.7.3C,D). In addition, clustering based on cellular compartments, reveals association of targets with axon, dendrites, synapse and post synaptic membrane (Fig.7.3E,F). This bioinformatics analysis suggests that a specific population of miRNAs translocates to mitochondria under FXTAS condition, and their targets are associated with mitochondria, brain and neuronal functions.

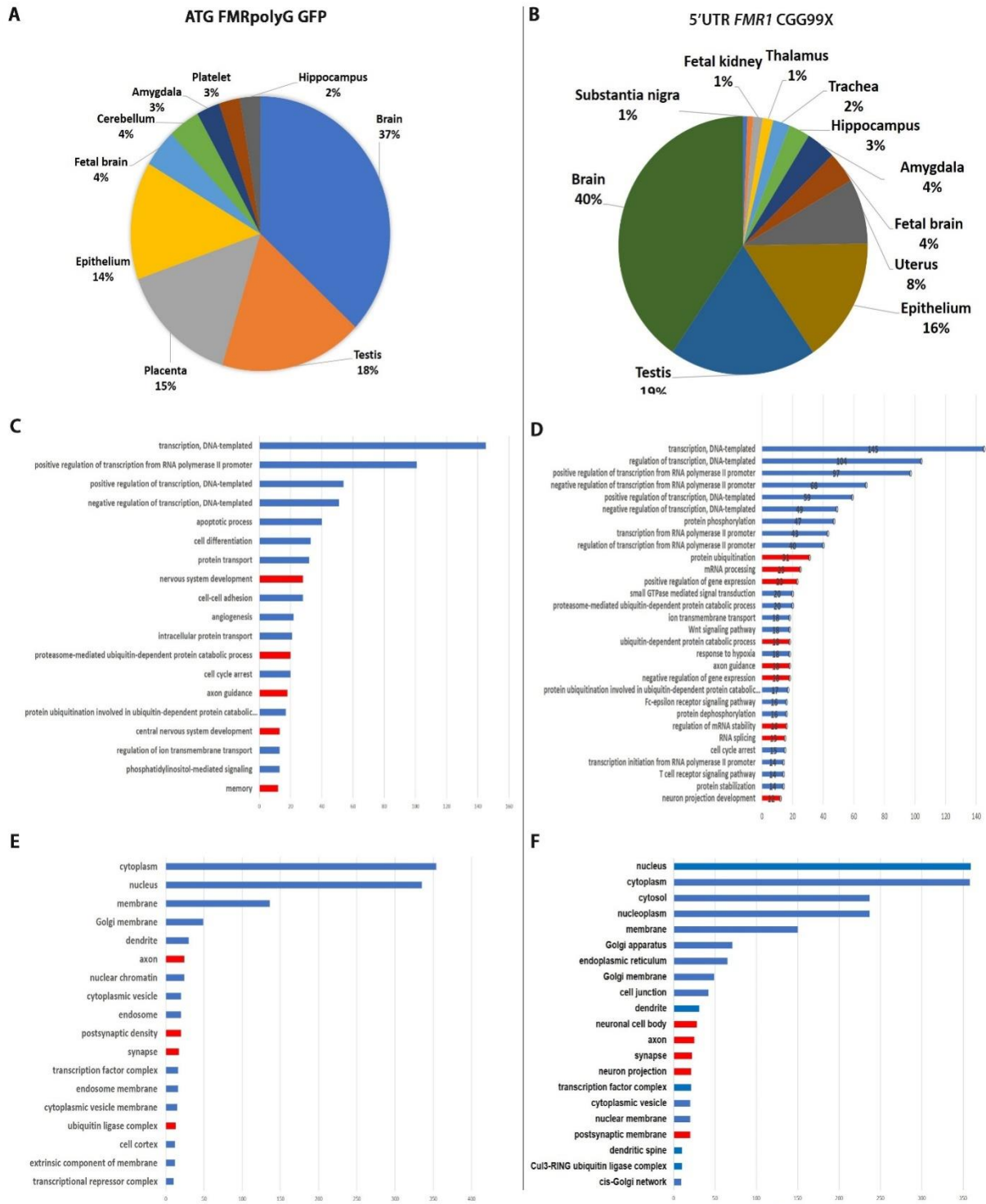


Figure 7.3. Bioinformatics analysis for targets of differentially associated miRNAs with mitochondria in expanded CGG repeats transfected conditions. Targets of miRNAs were predicted through miRDB and StarBase. DAVID platform was used for clustering of the targets into meaningful groups such as pathways involved, OMIM enriched tissue (A,B), biological process (C,D) and cellular compartments (E,F) using DAVID platform.

7.2 Mito-miR, miR-320a translocates to mitoplast in FXTAS condition

The differential pattern of association of miRNAs with mitochondria in premutation condition was further confirmed by RT-qPCR. U6 snRNA and 5S rRNA were evaluated for reference RNA and positive control for mitochondrial fraction as both of them have been reported to associate with mitochondria [11], [12]. We observed no change in the Ct values of 5S rRNA in mitochondria, cytosol and WCL between control and CGG repeats transfected groups. Ct values of U6 snRNA were notably altered in control and CGG repeats transfected groups in all subcellular fractions (Fig. 7.5A). 5S rRNA was used as reference RNA for several reasons as 5S rRNA has been known to be transcribed in the nucleus and transported to mitochondria and associates with mitochondrial ribosomes [13], [14]. Further, the miRNA of our interest, miR-320a is also nuclear encoded and transported to mitochondria under CGG repeat transfected conditions. Hence, to rule out any transport defect, 5S rRNA was selected as endogenous control to compare the change in expression levels of miRNAs under premutation condition for all subcellular fractions. Candidate miRNAs hsa-miR-181a, hsa-miR-221, hsa-miR-320a, hsa-miR-4485 and hsa-miR-148-3p were selected for their quantification in whole cell, mitochondria and cytosolic fractions from HEK293 cells transfected with ATG FMRpolyG-GFP, 5'UTR *FMR1* CGG99X and pEGFP-C1.

The selected miRNAs showed differential pattern of association with mitochondria as compared to their whole cell enrichment in premutation condition (Fig. 7.4A). We selected miR-320a for further exploration as this miRNA was previously reported as a mito-miR [7],[15], and its protective roles during cellular stress and a tumor suppressor have been reported in some studies [37],[38]. Submitochondrial localization of miR-320a was analyzed by isolating pure fractions of mitochondria, mitoplast and intermembrane space (IMS) and analyzing the level of miR-320a using qRT-PCR. Immunoblotting against TOMM20, a marker of the outer membrane protein showed high level in mitochondria and IMS fractions but not in mitoplast. AIF, a marker of the mitochondrial inner membrane was found in mitochondria and mitoplast, confirming the purity of the submitochondrial fractions (Fig.7.5B). The purity of submitochondrial fractions was further confirmed by estimating levels of different RNAs including actin (cytosol), COX1 (mitoplast) and miR-4485 (mitoplast, [1]). where corresponding low Ct value of actin in total cell

as compared to other sub mitochondrial fractions and low Ct values of COX1 and miR-4485 in submitochondrial fractions as compared to total cell suggest purity of submitochondrial fraction at RNA level (Fig. 7.5C). as miR-4485 and COX1 is localized to mitoplast they are used here to further confirm the purity of mitochondrial fraction,

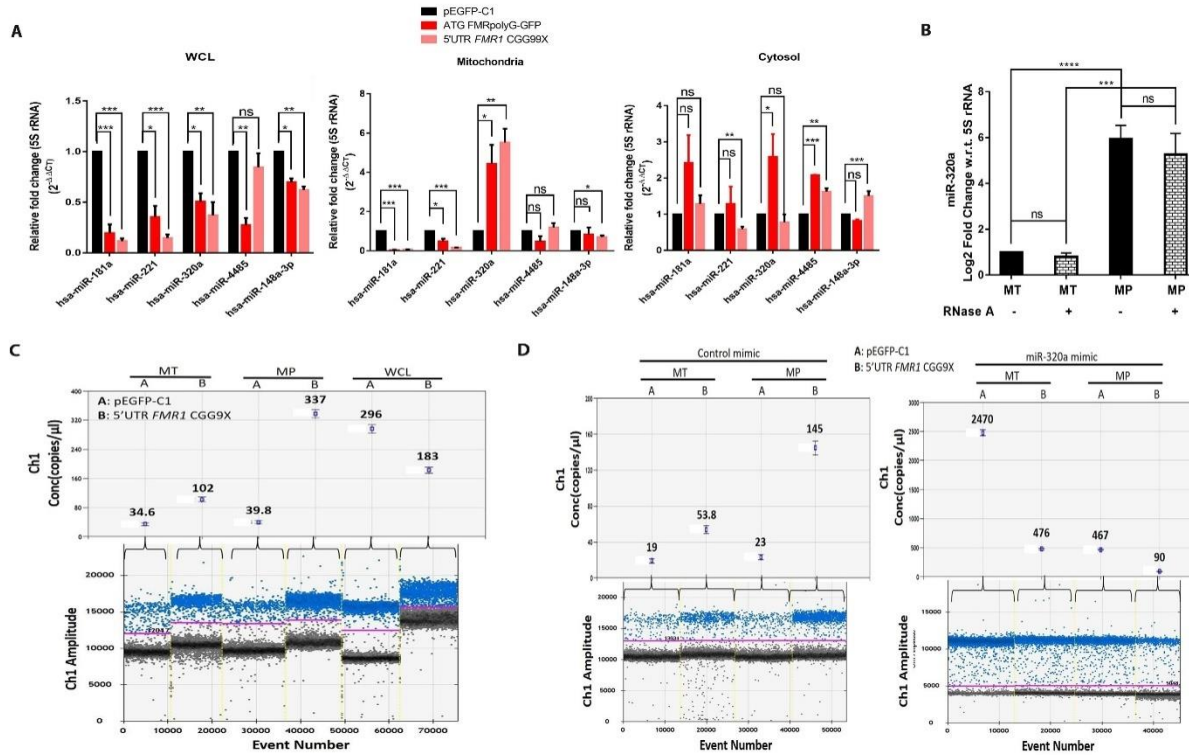


Figure 7.4. Validation of candidate miRNAs by qPCR and localization of miR-320a in mitoplast under premutation condition. Candidate miRNAs has-miR-181a, hsa-miR-221, hsa-miR-320a, hsa-miR-4485 and hsa-miR-148a-3p were screened from the next generation sequencing analysis and their sub cellular localization was checked in various compartments such as whole cell lysate (WCL), mitochondria and cytosol under both CGG repeats transfected condition (n=3, endogenous control: 5S rRNA) (A). Mitoplast fraction was prepared by treating mitochondria with digitonin and both mitochondrial and mitoplast fractions were treated with RNase A to confirm submitochondrial localization of miR-320a (n=3)(B). Digital Droplet PCR: droplet distribution and box plot representing enrichment of miR-320a in mitochondria (MT), mitoplast (MP) and whole cell lysate (WCL) under 5'UTR FMR1 CGG99X transfected condition compared to control (n=2, Blue : positive droplets, Grey : negative droplets, box plots represents concentration in copies/ul) (C). Enrichment of exogenously transfected miR-320a mimic at mitochondria and mitoplast represented as change in amplitude of positive droplets (blue) and altered copies/ul (box plot) under premutation condition (n=3) (D).

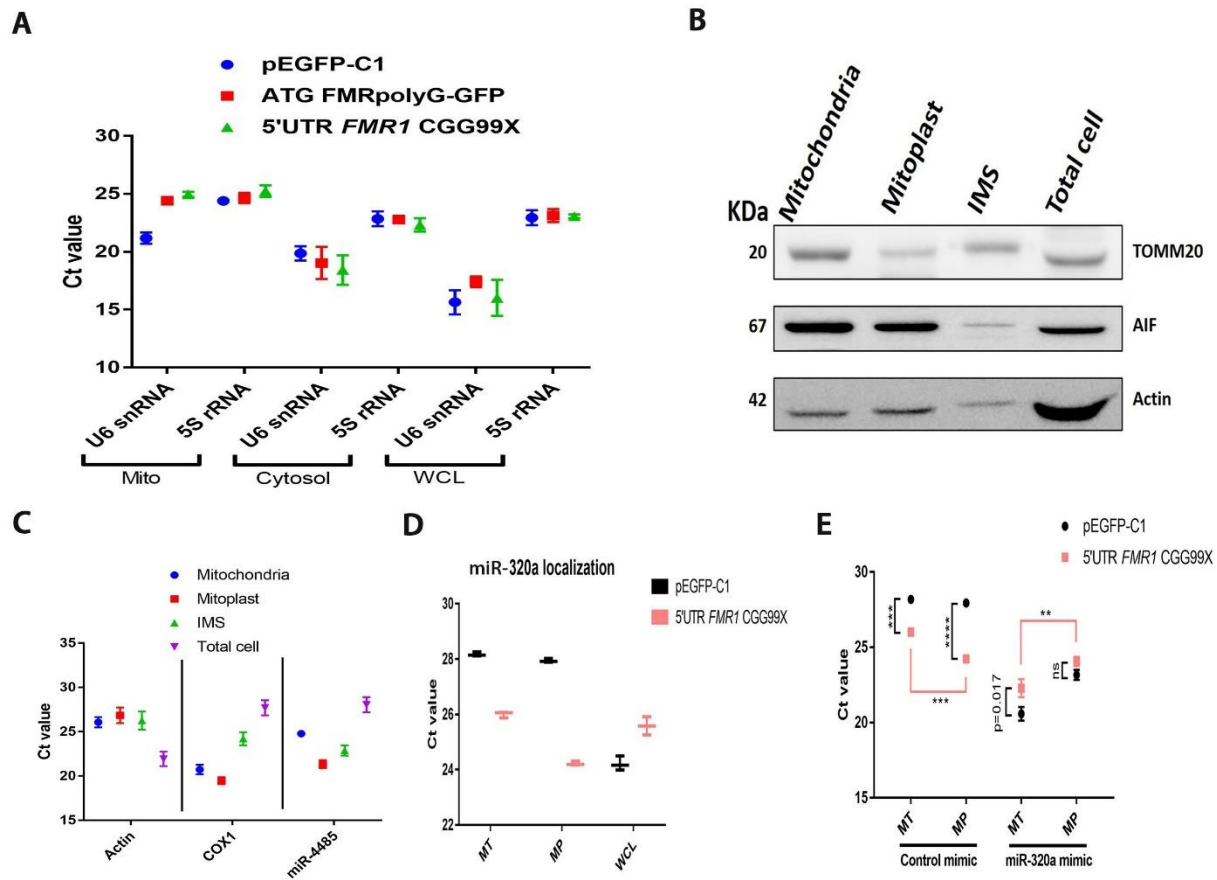


Figure 7.5. Validation of endogenous controls and mitoplasmic localization of miR-320a. qPCR analysis showing Ct values of U6 snRNA and 5S rRNA in mitochondria (Mito), cytosol and whole cell lysate(WCL) fractions of HEK293 cells expressing pEGFP-C1 and 5'UTR *FMR1* CGG99X (n=3)(A). Validation of purity of submitochondrial fraction by western blotting analysis: Increased level of AIF in mitoplast, absence of outer membrane protein marker TOMM20 in mitoplast and low expression of actin in submitochondrial fractions show less contamination from cytosol (actin) suggest high purity of submitochondrial fractions (n=3) (B). Purity of submitochondrial fractions confirmed at RNA level by qPCR and plotting corresponding Ct values for RNAs reported in mitoplast: COX1 and miR-4485 (n=3) (C). qPCR validation for mitoplasmic enrichment of miR-320a underCGG repeats transfected condition(plotted Ct values, n=2) (D). qPCR validation of submitochondrial localization of miR-320a in presence of miR-320a mimic under control and CGG repeats transfected groups (n=3) (E).

RNase A protection assay was performed with mitochondria and mitoplast fractions from HEK293 cells followed by RNA isolation. qPCR analysis showed high levels of miR-320a in RNase A treated mitoplasts and was not degraded upon treatment with RNase A suggesting its localization in mitoplast (Fig.7.4B).

ddPCR can determine copy number of RNA accurately and has been proved to be more tolerant to the presence of inhibitors of the amplification reaction compared to qPCR [18]. These properties of ddPCR have made it useful for detection of cellular and circulating miRNAs [19]. We performed ddPCR to further quantify the changes in abundance of miR-320a in mitochondria, mitoplast and whole cell fractions. Increased number of positive droplets (blue) and more copies/ μ l of miR-320a was observed in mitochondria and mitoplast fraction in 5'UTR *FMR1* CGG99X transfected condition as compared to pEGFP-C1 (Fig. 7.4C, 7.5D). The results were consistent with RT-qPCR results as observed in Fig. 7.4A. Furthermore, ddPCR confirmed decreased levels of miR-320a under premutation conditions in whole cell lysate (Fig. 7.4C). These results suggest that expression of CGG repeats may either induce degradation of miR-320a within the cytoplasm and/or enhance its translocation to mitochondria, inside the mitoplast. To discriminate between these hypothesis, we transfected HEK293 cells with a synthetic mimic of miR-320a along with a control for both pEGFP-C1 and 5'UTR *FMR1*CGG99X transfected conditions. The transfection of miR-320a mimic in cells showed enhanced localization of miR-320a in mitochondria as well as in mitoplast in 5'UTR *FMR1*CGG99X condition as compared to control (Fig. 7.4D, 7.5E). Here, we observed that high proportion of endogenous miR-320a is enriched in mitoplast in control mimic transfected conditions in 5'UTR *FMR1*CGG99X transfected cells. Although, cells expressing 5'UTR *FMR1*CGG99X along with miR-320a mimic showed high copies/ μ l in mitochondria but the pattern of miR-320a translocation to mitochondria/mitoplast was not the same as observed in control mimic condition. Overall, these results suggest that miR-320a translocates to mitochondria and resides in mitoplast and this transport is enhanced in FXTAS condition.

7.3 miR-320a binds to Ago2 and mitochondrial transcripts in mitochondria

The mitoplast enrichment of miR-320a suggest that it may regulate mitochondrial transcripts processing and/ or translation. Therefore, to identify the role of miR-320a inside the mitoplast, we searched for putative targets of miR-320a by miRDB and StarBase. The list of potential mRNAs targeted by miR-320a comprises various nuclear encoded mitochondrial proteins, including EARS2, GLUD1, COX11, SDHC, SDHD, NDUFS1 and NDUFA10 (Table 7.1).

Interestingly, we also identified putative miR-320a targets which includes mitochondrial transcripts 16S rRNA, ND1, COX1, ND4, CytB and ND5 using BLASTn tool (Fig 7.6).

Table 7.1. Targets of miR-320a predicted by miRDB and StarBase

S. No.	Cluster Id	Putative Targets
1	Mitochondria	SLC9A6, TUSC3, TMEM143, GOT2, ACBD3, TBC1D15, UQCR11, AGPS, STARD7, COL4A3BP, TRAK1, DNAJC5, ELOVL6, HADH, TMEM14C, MTO1, MRPL35, GATM, FAM82A2, LYRM4, MTPAP, CLPX, EARS2, LETM1, GLUL, MRPS18B, C3ORF1, SLC25A33, SLC25A36, MRPL49, NEK9, ATP1F1, TFB1M, AKAP1, MTFMT, MRPL43, CAV2, MCL1, GLUD1, WARS2, CTSA, SFXN1, TK2, MUT, MTCH1, QTRTD1, C2ORF56, PEMT, GPD2, MRPS22, MRPS25, TAOK3, LACTB2, VDAC1, OCIAD2, SLC25A12, DNA2, SLC25A13, TOMM70A, HEBP1, ASAH2B, FOXRED1, ZFH3, MRP63, ARSB, E2F1, COX11, COX10, BNIP3, HLCS, PTEN, ARL2BP, ACN9, MTRF1, ASAH2, CDS2, MCCC2, TRIAP1, GSR, ACOT7, CASP3, AGPAT5, FRMD6, TPP1, DNAJC11, CASP7, ATP5L, ABHD10, SUCLA2, NDUFS1, TOMM34, BRD8, PRKCA, FUNDC2, MRPS5, DARS2, NDUFA10, COQ5, MTRR, ACADVL, TRAP1, ATP6V1A, MFN1, PANK2, PSEN1, PGS1, YWHAZ, ADH5, ATP5G1, NR3C1, COX7A2L, ATP5G3, TSC22D3, SH3GLB1, BCL2, PPP2CA, CSDE1, PPP3CB, PPP3CA, ACSL4, TXNIP, PDK1, DLST, VHL, CS, KIAA1967, ILF3, XPNPEP3, YWHAE, MSRB3, CAPRIN2, TFRC, SDHC, GOLPH3, BNIP3L, SDHD, WHSC1L1, NLN, SCP2
2	Cancer	E2F1, E2F3, MITF, FOXO1, GLI2, PTEN, CTNNA1, MAX, CASP3, RHOA, PIK3CA, AKT3, PRKCA, CTBP1, RALBP1, RELA, LEF1, FADD, CDK6, RB1, MECOM, STK4, RAD51, MAPK1, HIF1A, MAPK9, LAMC1, PIAS1, XIAP, GRB2, KITLG, ITGB1, IGF1R, BCL2, SOS2, RAC1, TRAF6, RUNX1, PIK3R3, PIK3R1, APC, PIK3R2, MSH6, DVL3, COL4A1, MSH3, VHL, MSH2, TGFBR1, CBL, TGFBR2, SMAD4, STAT1, APPL1, STAT3, RASSF5, HDAC2, GSK3B, CRK

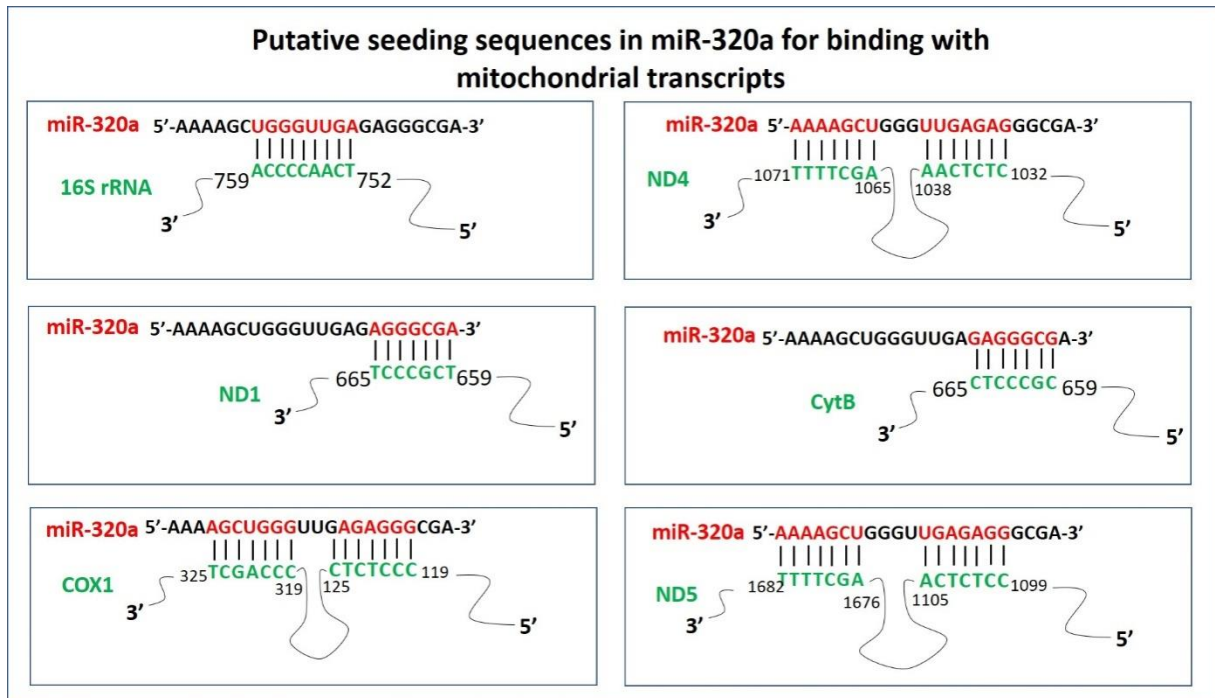
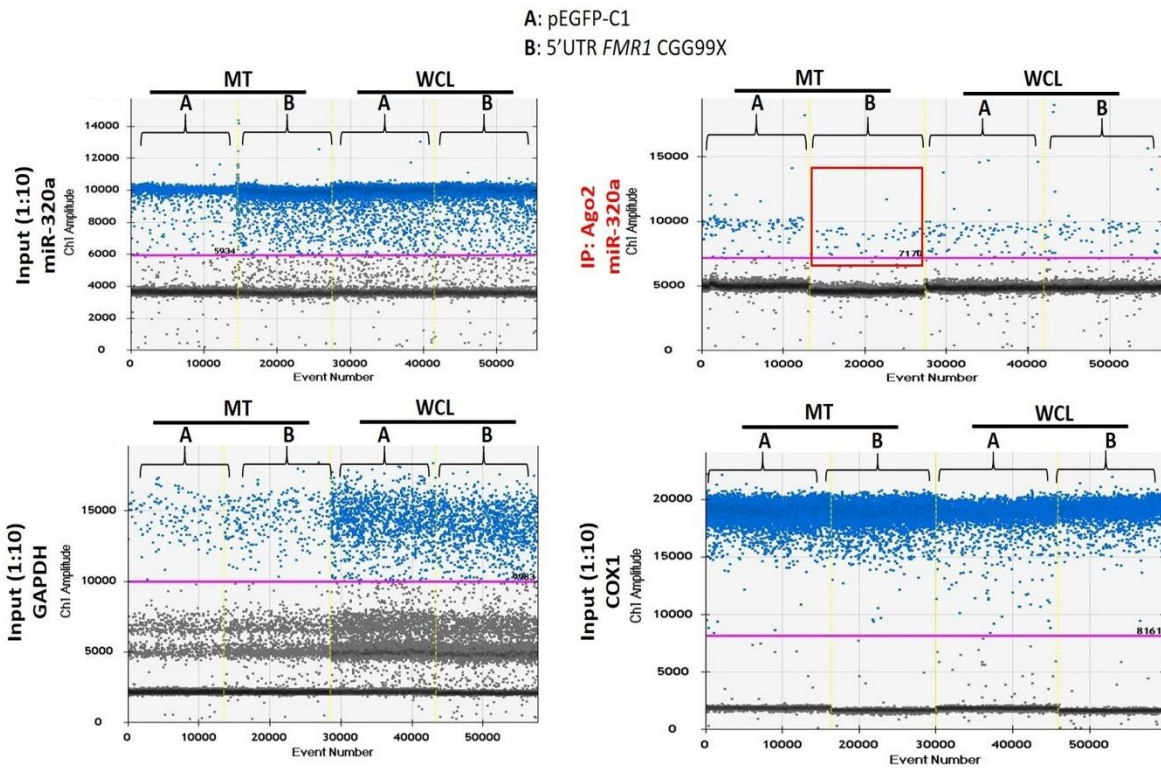


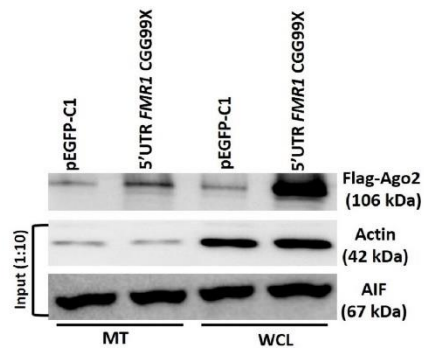
Figure 7.6. Putative seeding sequences (7-8mers) present in miR-320a (red) which can interact with 3' region of mitotranscripts (green) identified by BLASTn tool.

Ago2 is an essential component of RISC and growing evidences suggest the presence of Ago2 inside mitochondria, where it may regulate expression of some mitochondrial transcripts [20]–[22]. Thus, to test whether miR-320a may assemble in a RISC-like complex with Ago2 and regulate mitotranscripts, we first tested the possible binding of miR-320a with Ago2 by RNA-immunoprecipitation assay followed by ddPCR. Analysis of RNA-IP showed less population of miR-320a positive droplets (blue) (Fig. 7.7A) and decreased copy number/ μ l (Fig. 7.8A) in the mitochondrial fraction of CGG repeats transfected cells as compared to control. Similar results were obtained by RT-qPCR (Fig.7.8B). COX1, which is mitochondrial genome encoded transcript was used as endogenous control as well as reference RNA to check purity of mitochondrial fraction. COX1 has already been shown no change in its levels upon expression of expanded CGG repeats in HEK293 cells[23]. High abundance of positive droplets of COX1 (input) and very low amount of GAPDH (input) positive droplets confirmed purity of mitochondrial fractions. Interestingly, immunoblotting analysis showed increased level of Ago2 in total cell lysate as well as in mitochondria in the cells expressing of 5'UTR *FMRI* CGG99X (Fig. 7.7B).

A



B



C

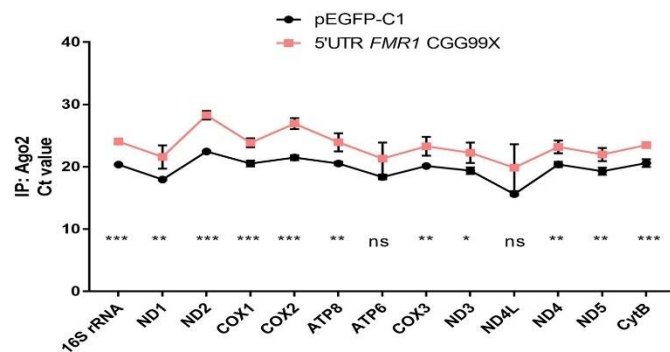


Figure 7.7. miR-320a regulates levels of mitochondrial transcripts by modulating RISC assembly with Ago2 and mitotranscripts. Flag-Ago2 cotransfected with expanded CGG repeats and control. Equal amounts of purified mitochondria and whole cell lysate (WCL) were subjected to RNA immunoprecipitation using anti-flag beads. Population of miR-320a bound to Ago2 was determined using ddPCR. 1D plot for droplet distribution (A) indicates levels of miR-320a bound with Ago2 in pre-mutation condition in both the fraction. Input (1:10) was analysed for reference gene of mitochondria (COX1) and WCL (GAPDH) and to detect endogenous miR-320a levels. Western blotting data showed specific anti-Ago2 IP blotted against flag antibody where Input (1:10) was probed against actin and AIF antibody for validation of mitochondrial fraction (B). Individual mitochondrial transcripts bound to miR-320a from RNAs of Ago-IP were examined by qPCR (plotted respective Ct values) (C). (n=2) $p > 0.05$ (ns), $p \leq 0.05$ (*), $p \leq 0.01$ (**), $p \leq 0.001$ (***)

Finally, RT-qPCR of various mitochondrial transcripts were performed using RNAs of Ago2-IP from the mitochondrial fraction to estimate the levels of mitotranscripts bound to Ago2 upon expression of 5'UTR *FMR1* CGG99X as compared to control pEGFP-C1. The higher Ct values for majority of mitochondrial transcripts revealed a decreased binding of mitotranscripts with Ago2 in premutation condition as compared to control (Fig. 7.7C). Collectively, our data suggests an increased translocation of miR-320a as well as of Ago2 into mitochondria under premutation condition; however, this does not result in assembly of a functional RISC like complex.

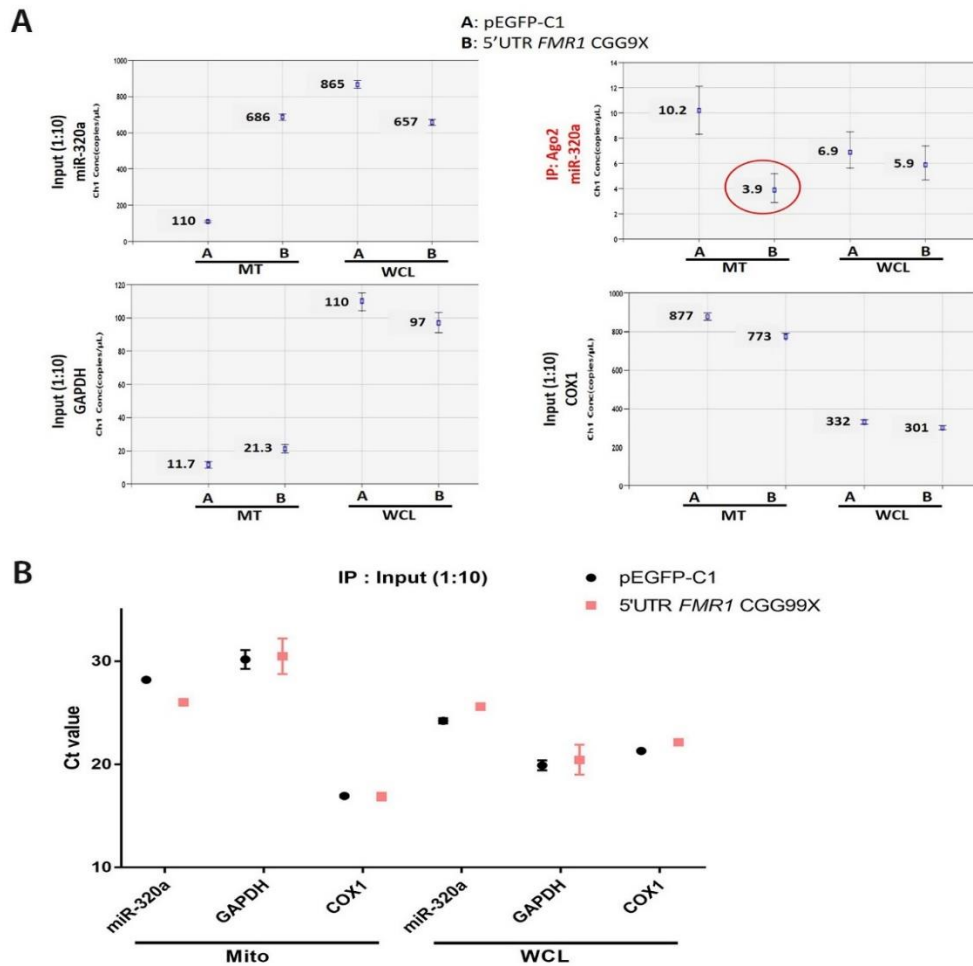


Figure 7.8. Interaction of miR-320a with Ago2 gets altered under premutation condition. ddPCR: box plot indicating levels of miR-320a bound with Ago2 (copies/ μ l) under premutation condition in mitochondria and WCL fraction (marked red) along with endogenous controls for mitochondria (5S rRNA), WCL (GAPDH) and endogenous miR-320a levels of input (1:10) (n=3) (A). RNAs isolated from Input (1:10) of Ago2-IP were further analysed by qPCR to quantify Ct values for endogenous miR-320a, GAPDH and COX1 (n=3) (B).

7.4 miR-320a improves mitochondrial transcripts levels and mitochondrial functions in FXTAS conditions

To understand the impact of the decreased binding of miR-320a with Ago2 on mitochondrial functions, we first quantified the level of mitochondrial transcripts in FXTAS condition. The expression of 5'UTR *FMRI* CGG99X showed decreased levels of mitotranscripts (Fig 5A), which is consistent with previous reports [24],[25]. Interestingly, we observed a rescue in levels of majority of mitotranscripts in presence of miR-320a mimic (Fig. 7.9A). Next, we explored the effect of CGG repeats and miR-320a on the activity of mitochondrial respiratory chain. Briefly, HEK293 cells were transfected with pEGFP-C1 and 5'UTR *FMRI* CGG99X along with miR-320a mimic and mitochondrial fractions were isolated. BN PAGE was performed followed by in-gel staining for complex I and IV. Expression of the CGG premutation significantly decreased complex I (NADH dehydrogenase) and complex IV (Cytochrome Oxidase) activities compared to control condition (Fig. 7.9B). Importantly, cotransfection with miR-320a mimic corrects the deleterious effect of the CGG repeats on complex IV activity (Fig. 7.9B). Further, transfection of miR-320a mimic enhanced the level of ATP in cells expressing 5'UTR *FMRI* CGG99X (Fig. 7.9C). Finally, we examined cellular ROS levels by DCFDA staining where rotenone (25 μ M for 2 hours) treated group taken as positive control. The increased ROS levels in premutation condition was not statistically significant; however, cotransfection with miR-320a mimic caused decreased levels of cellular ROS under 5'UTR *FMRI* CGG99X (Fig. 7.9D). Combining all the results, it can be inferred that miR-320a can rescue some of the mitochondrial dysfunctions in FXTAS condition.

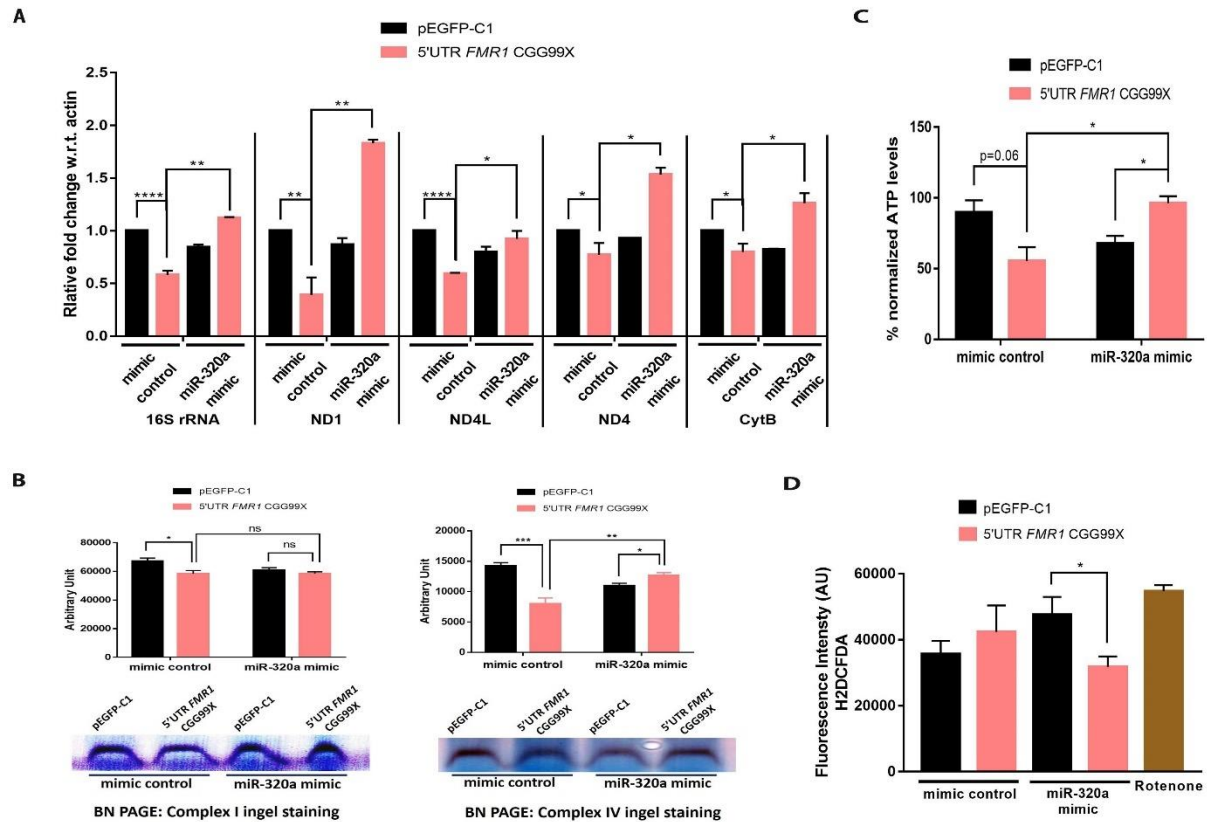


Figure 7.9. Transfection of miR-320a rescues mitochondrial transcripts and mitochondrial functions in FXTAS. HEK293 cells transfected with miR-320a mimic along with 5'UTR *FMR1* CGG99X and pEGFP-C1. After 24 hours of transfection, various mitochondrial functions was analysed. qPCR results showing levels of mitochondrial transcripts (n=4) (A). Effect of miR-320a mimic on activity of mitochondrial complex I and IV determined by BN PAGE followed by ingel staining (includes densitometry analysis, n=3) (B). ATP levels were also monitored within same groups (n=3) (C). Cellular ROS levels were determined by staining the cells with H2DCFDA and fluorescence intensity was plotted for each group (n=3, Rotenone; positive control) (D). $p > 0.05$ (ns), $p \leq 0.05$ (*), $p \leq 0.01$ (**), $p \leq 0.001$ (***)

7.5 miR-320a improves cell survival in FXTAS condition

To investigate whether the improved mitochondrial functions mediated by miR-320a also impacts cell viability, HEK293 cells were co-transfected with plasmid 5'UTR *FMR1* CGG99X along with miR-320a mimic followed by propidium iodide (PI) and MTT staining. Importantly, 5'UTR *FMR1* CGG99X cotransfected with miR-320a mimic showed decreased level of PI fluorescence, indicating decreased cell death as compared to CGG repeats transfected with control mimic (Fig. 7.10A). Similarly, MTT assay indicated increased cellular viability in presence of miR-320a mimic in CGG repeat transfected cells (Fig. 7.10B). We also monitored PARP cleavage and

caspase activation by western blotting. As expected, increased PARP and caspase 3 cleavage were observed in premutation conditions which is in consonance with earlier findings[25], [26]. Further, the level of cleaved PARP and active caspase 3 decreased in cells expressing CGG repeats in presence of miR-320a mimic(Fig. 7.10B). Collectively, these data indicate that miR-320a can improve cell viability in *in vitro* cellular model of FXTAS.

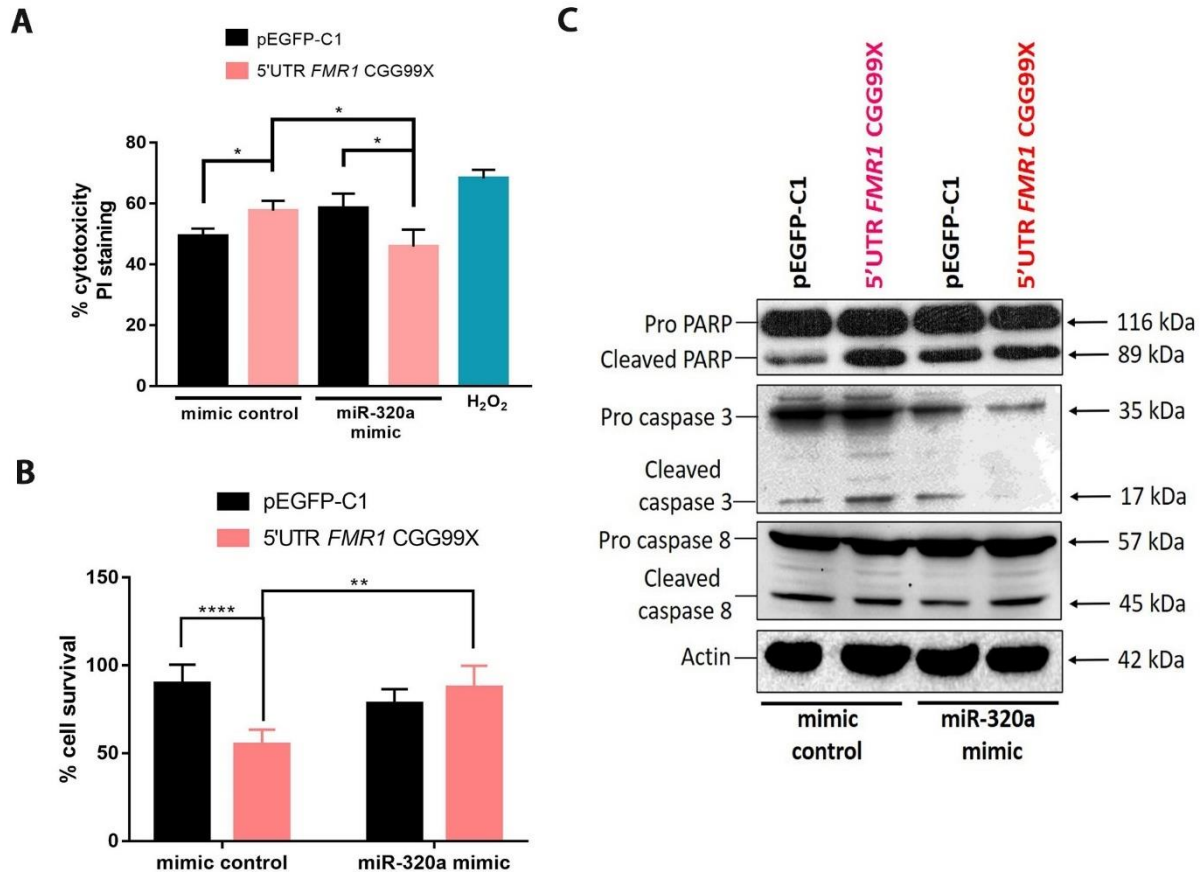


Figure 7.10. miR-320a causes decreased cellular ROS levels and increased survival in premutation condition. Cytoprotective role of miR-320a was analysed by transfecting miR-320a under CGG repeats expressed condition together with respective controls in HEK293 cells. PI staining was performed to assay population of cells undergoing apoptosis (n=3, H₂O₂:positive control) (A). Recued cell death and increased cell survival was investigated by MTT assay (n=3) (B). Western blotting was performed by probing and detecting the samples against different apoptotic markers such as caspase 3, caspase 8 and PARP (n=3) (C). p > 0.05 (ns), p ≤ 0.05 (*), p ≤ 0.01 (**), p ≤ 0.001 (***)

7.6 Discussion

Mitochondrial dysfunction is a key pathogenic event reported in FXTAS cellular and animal models and premutation carriers [24], [25], [27]–[29] however, the molecular mechanism causing such mitochondrial dysfunctions in FXTAS remain to be determined. The plausible hypothesis behind such mitochondrial dysfunctions can be titration of DROSHA and DGCR8 by the expanded CGG repeats RNA resulting in decreased miRNA biogenesis. This is consistent with our miRNA expression data in FXTAS patients, where we observed decreased miRNA levels in RNAs derived from brain tissue of premutation carriers. Furthermore, FMRP, the protein encoded by *FMR1*, is known to regulate mRNA translation via interacting with Dicer in the RISC. Therefore, decreased levels of FMRP observed in premutation carriers may also affect miRNA function by altering RISC activity [30],[31].

In the previous chapter, we reported that FMRpolyG transiently interacts with mitochondria and alter mitochondrial functions [25] and an earlier mass spectroscopy analysis of FMRpolyG interacting proteins identified several proteins important for nuclear-cytoplasmic trafficking but also for mitochondrial RNA processing (FASTKD5, DHX30) [2]. This suggests that FMRpolyG may not only alter pre-miRNAs export from the nucleus, but also proteins important for the import and processing of mRNAs within mitochondria. This hypothesis is in consonance with our current work where we observed decreased cellular miRNAs and their altered translocation to mitochondria. This may have large pathogenic consequences, as bioinformatics analysis indicated that targets of identified mito-miRs are involved in regulation crucial neuronal and mitochondrial functions; however, this hypothesis needs to be formally addressed, especially as the molecular mechanism for transport of miRNAs to mitoplast is unclear [32].

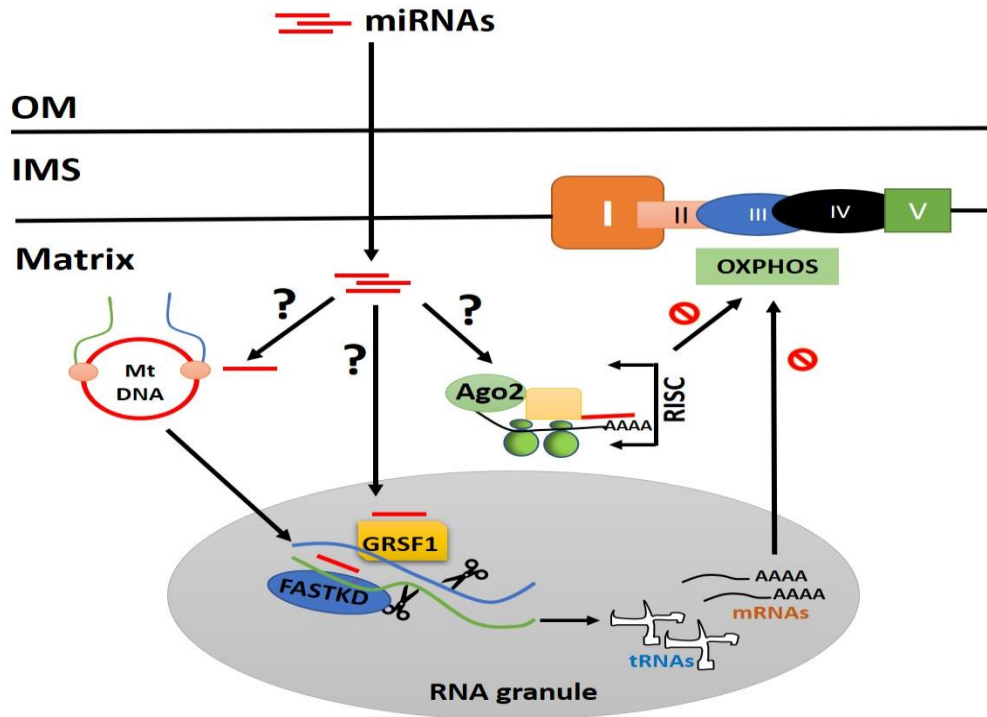


Figure 7.11. Schematic representation of different pathways by which miRNA present in mitochondrial matrix can regulate mitochondrial RNA processing and ultimately mitochondrial transcript levels.

Our group has previously reported that miRNAs can translocate to mitochondria under different patho-physiological stimuli [15],[42]. The transport of nuclear encoded miRNAs to the mitochondria is required for optimal mitochondrial function [11],[22]. There can be multiple pathways by which miRNAs residing in mitochondria can regulate mitochondrial functions. First, miRNAs can directly bind to mito-DNA and can regulate transcription of mitogenome [15],[33]. Second, miRNAs can affect RNA processing causing RNA interference by binding to immature mitotranscripts [1]. Third, miRNAs can regulate translation of mature transcripts by forming RISC like assembly with Ago2 within mitochondria and facilitates with mito-ribosome scanning [22],[34]. The evidences here along with previous reports strengthen the hypothesis of presence of Ago2, component of RISC inside the mitochondria; while presence of other subunits of RISC complex have not been explored in the FXTAS conditions. Interestingly RNA-IP with Ago2 showed miR-320a interaction with mitochondrial transcripts supports the earlier findings claiming Ago2 binds to miRNA-mito transcripts and regulate the mitochondrial translation [22].

We identified a population of miRNAs which is highly enriched in mitochondrial fraction due to cellular stress induced by expression of 5'UTR *FMR1*CGG99X which might be help in rescuing mitochondrial functions. Among these miRNAs, we characterized miR-320a for its functional role in FXTAS. RNase A protection assay along with ddPCR confirmed the presence of miR-320a within mitoplast. RNA-IP with Ago2 suggest decreased binding of miR-320a with mitochondrial transcript and Ago2 in FXTAS condition. Interestingly, transfection of miR-320a mimic positively modulates mitotranscripts processing and ultimately restores mitochondrial functions in premutation condition. This suggests that miRNA-mitotranscripts interaction with Ago2 and may regulate the level of mitochondrial DNA encoded proteins in narrow physiological range for maintaining optimal functions. This study further suggests that specific population of miRNAs can associates with mitochondria in complicated pathology like FXTAS and other chronic neurodegenerative conditions.